ELSEVIER

Applied Surface Science 94/95 (1996) 148–155

applied surface science

Laser photoelectron projection microscopy with subwavelength spatial resolution

V.N. Konopsky, S.K. Sekatskii *, V.S. Letokhov

Institute of Spectroscopy, Russian Academy of Sciences, Troitsk, Moscow region 142092, Russia

Received 3 October 1995; accepted 3 October 1995

Abstract

The development of a laser photoelectron projection microscope with a magnification up to 10^5 and spatial resolution up to 30 nm as well as the first results of studies of needle tips made of LiF crystals with F_2-aggregated centers with the use of this microscope are reported. The resolution achieved was sufficient to visualize individual defects on the crystals surface. The effects of thermal faceting of LiF:F_2^- needle tips due to their heating by intense laser radiation were observed for the first time.

1. Introduction

The photoelectron microscopy method, whereby the image of a cathode produced by the electrons emitted from its surface under the effect of light in the visible, UV or X-ray regions of the spectrum is recorded at a high magnification, is a valuable research tool in metallurgy, surface physics, microelectronics, biology, etc. [1]. The potentialities of this method and the domain of its application can be widened considerably if it will be possible to observe and interpret the photoelectron images formed by the action of laser on the samples [2,3]. Choosing different objects of investigation and appropriate methods of their laser irradiation one can hope to solve such fundamental problems as visualization of chromophores in complex organic molecules [2], determination of the arrangement of single impurity ions or color centers in dielectric crystals [3], visualization of small light absorbing inhomogeneities in transparent samples [3], etc. For the registration of the coordinates of the photoelectron emitted both versions of photoelectron microscopy technique can be applied – its classical version based on the resolution of the coordinates of the emitting center by electron optics and the projection lensless version based on the possibility of studying tips with a very small radius of curvature r with a high spatial resolution.

The first successful realization of a laser photoelectron projection microscope is reported in this paper. LiF crystals with F_2-aggregated centers were used as an object of investigation in the experiments. This choice was initiated by the following factors.

First, for wide-gap ionic crystals the external photoelectric effect has been studied in a number of works that has permitted to establish its main charac-

* Corresponding author. Fax: +7 095 334 0886; e-mail: lls@isan.msk.su.

SSDI 0169-4332(95)00363-0

teristics and among them its "selective" character: when wide-gap crystals are irradiated by visible or UV light, the observed photoemission is caused by the photoionization of different defects or impurities in these crystals and not by the photoionization of the crystal matrix (see Ref. [4] and the references cited therein, as well as Refs. [5,6]). Thus, choosing proper samples of ionic crystals and the conditions of their laser irradiation one may hope for successful visualization of single defects in these crystals that would clearly demonstrate the chemical selectivity of the method. Besides, since the defects concentration may be much less than the density of atoms in the crystal lattice, an ultrahigh atomic spatial resolution is not necessary for successful solution of the problem. It should be also noted that recently we have established concrete mechanisms and the conditions for realizing the selective two-step external photoelectric effect for color centers in LiF crystals [5,6].

On the other hand, the visualization and investigation of defects in LiF crystals are of great independent importance since LiF crystals with color centers are widely used as a material for quantum electronics and in ionizing radiation control [8,9].

2. Laser photoelectron projection microscope

The scheme of laser photoelectron projection microscope is given in Fig. 1. The microscope needles were made of LiF:F_2 crystals synthesized at the Institute of General Physics, Russian Academy of Sciences, Moscow, by etching crystal fragments in concentrated hydrochloric acid solution. The elaborated etching technique made it possible to fabricate needles several millimeters long, their tips being nearly conical with the radius of curvature r of up to $\simeq 600$ nm and the vertex angle of several degrees. Wood's alloy was used to fasten the needles to an electrode supplied with a constant voltage V, within 0 up to -2.5 kV when photoelectron images of needle tips were observed or up to $+20$ kV when we

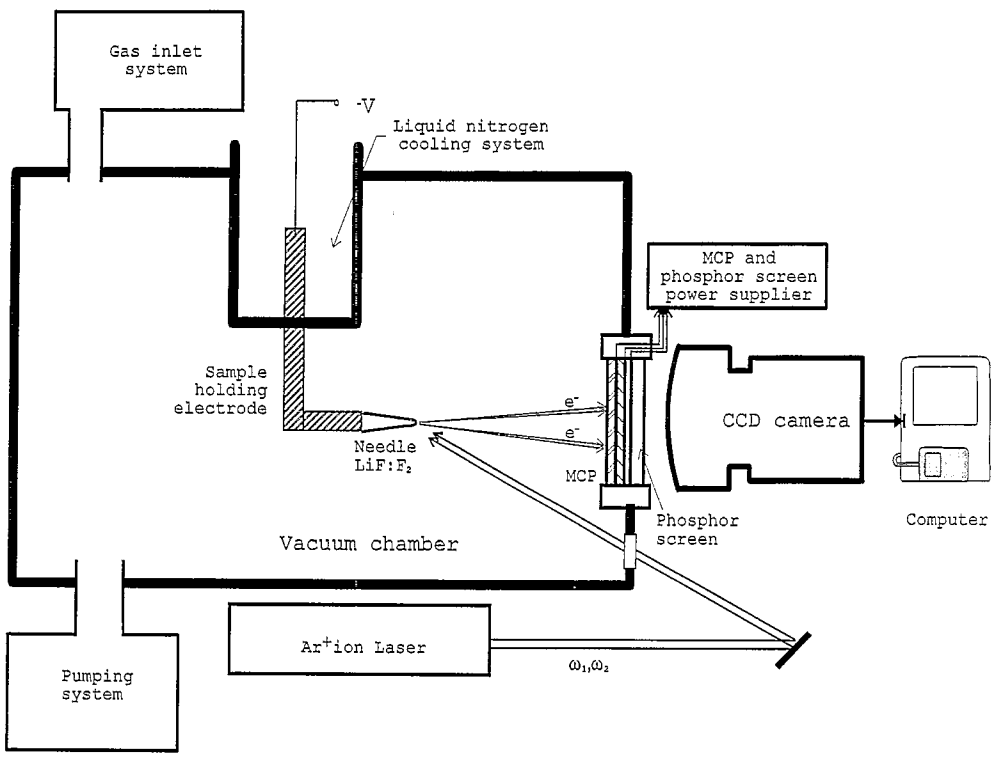

Fig. 1. Scheme of the laser photoelectron projection microscope.

observed the images of the needle tip, produced by the positive ions desorbed from the needle surface. A lens with its focal length of 17 cm focused the Ar^+ laser (Model 2020, Spectra Physics) radiation onto the needle tip. In our experiments we applied different types of laser radiation focusing; some experiments were performed without a focusing lens with the unfocused laser beam. The needle tips were irradiated by all Ar^+ ion laser spectral lines (in most cases), as well as separately at the lines 488 and 514 nm, and also using light filters cutting off the violet and UV regions of Ar^+ laser radiation. The photoelectrons emitted from the needle tip were directed by electric field to the grounded input of the microchannel plate and luminescent screen assembly 10 cm distant from the tip. The optical image formed at the assembly output was taken by a TV camera connected to a specialized image processing computer system (Argus-50, Hamamatsu Photonics, K.K., Japan). The angle of photoelectron collection was depended on the dimensions of the working region of the microchannel plate (diameter 32 mm) and was $\sim 20°$ so that only a small part of the tip could be observed in the experiment.

The investigations were carried out in a vacuum chamber equipped by a system for cooling the samples to the temperature of liquid nitrogen and a gas inlet system for observing the FIM images of needle tips. An oilless vacuum was kept in the chamber at 3×10^{-7} Torr level.

The methods of field electron microscopy (FEM) and field ion microscopy (FIM) at present are valuable research methods of obtaining information on the structure and properties of various surfaces of metal and semiconductor needle tips and atoms and molecules adsorbed on them (see Refs. [9–12]). As for the possibilities of this method to study insulating samples, this problem is not fully investigated despite some successful attempts in this direction, see for example Ref. [13]. The following considerations can be applied to the matter.

The resistance R of a dielectric needle between its contact point with a metal electrode (Wood's alloy) and its tip, from which electrons are emitted, can be estimated from the formula

$$R \simeq \rho \frac{1}{\pi \tan \vartheta} \frac{1}{r_0}, \qquad (1)$$

where 2ϑ is the vertex angle of the conical part of the needle; ρ is the specific resistance; r_0 is a some effective dimension of the region emitting photoelectrons. Eq. (1) shows that the main contribution to the resistance is made by the conical part of the needle and even only the part immediately adjacent to the tip. When r_0 is equal to the typical radius of curvature of the tip, i.e. 1 μm, and $\tan \vartheta \simeq 0.1$, it is easy to calculate R, which equals $3 \times 10^4 \rho$. To provide reliable recording of photoelectrons by MCP, it is necessary that they should be emitted with the potential being no higher than ~ -100 V, i.e. the maximum permissible voltage drop across the needle from the point of its contact with the Wood's alloy (at the potential of -2.5 kV) to the tip can be estimated to 2 kV. For the typical photoemission current of 10^{-13} A this is possible if the needle resistance does not exceed $\sim 2 \times 10^{16}$ Ω and hence the specific resistance of the needle material ρ must not exceed $\sim 10^{12}$ Ω cm. This estimate is still one or several orders of magnitude lower than the specific resistance of good insulators at room temperature. It should be noted, however, that the surface conduction is not taken into account here even thought it is known to be important for real dielectric samples. The conduction value may also depend on various effects conditioned by the strong electric field of the projection microscope in the vicinity of the needle tip as well as effects caused by the possible photoconduction of the material of the tips under laser irradiation. It must be also noted that for many insulators comparatively small heating is often sufficient to increase their conduction by many orders of magnitude. For example, the specific resistance of nominally pure LiF crystals at the temperature $T \simeq 250$°C lies in the range 10^8 to 10^9 Ω cm [14]. Simple estimations (in the frame of a one-dimensional heat conductivity model) show that, especially in the case of $LiF:F_2^-$ crystals, the samples in the experiments could be heated, in principle, by tens and hundreds of K under laser irradiation.

Thus, the estimates presented show that in many cases it is quite possible to produce photoelectron images of dielectric needles. This possibility is best illustrated by the photoelectron images of $LiF:F_2$ and $LiF:F_2^-$ needle tips obtained by us in experiments with a high spatial resolution. To avoid the space charge effects we worked in regime of very weak

(usually below 1 pA) currents. For such regime no difficulties associated with the charging of the samples were observed in these experiments.

When interpreting the photoelectron images of dielectric needles we used the same formulas as applied to analysis of the performance of electron and ion projectors with the metal needles [9–12]. The magnification of the photoelectron projection microscope was determined as

$$M = \frac{R}{\chi r}, \tag{2}$$

where χ is a numerical coefficient varying between 1.5 and 2. The electric field on the needle tip surface was estimated from the formula

$$E = \frac{U}{kr}, \tag{3}$$

where U is the tip potential, k is a numerical coefficient lying in the range 5 to 7. For a needle with the radius of curvature $r \simeq 600$ nm the application of these formulas gives the magnification $M \simeq 10^5$ and the electric field strength $E \simeq 0.08$ V/Å.

When investigating processes of photoemission from needles one should pay attention to the conditions on the surfaces under study since the presence of certain impurities on them may strongly affect the characteristics of photoemission and may lead to misinterpretation of the obtained results. In our experiments we controlled the tip surface conditions by observing the needle tip images formed by the positive ions desorbed from their surfaces. In this case a voltage of the opposite polarity (up to +20 kV) was applied to the needle and the photoion images resulting from the irradiation of the tips were analyzed. The rather large (50 to 100 nm), bright and unstable spots observed in this case were interpreted by us, in analogy with the practice of FIM with metal needles [10–12], as an indication of contamination of the surface by adsorbed molecules. By increasing the laser radiation intensity we could change the pictures observed. We began to observe quasiuniform illumination of the screen without a well-defined structure, and the integral photoemission intensity was much lower than that observed in the case of bright unstable spots. Most likely this shows that the surface was cleaned due to photostimulated desorption of the contaminations. As a rule, in this case it was necessary to expose the tip to laser radiation with an intensity of 2 to 6×10^3 W/cm^2 during several seconds. Just after such cleaning we reversed the voltage polarity on the needle and began to register the photoelectron images of the tip maintaining such laser radiation intensity that was sufficient to clean the surface. The experiments demonstrated a high stability and reproducibility of the images observed.

3. Photoelectron images of dielectric needle tips and their discussion

3.1. LiF:F_2 needles

Fig. 2 shows typical photoelectron images of LiF:F_2 crystal needle tips. Such images consisting of distinct dark and bright spots were observed by us for various LiF:F_2 needles and conditions of their laser irradiation. They could be observed, however, only in a comparatively narrow laser irradiation intensity range. For example, the intensity range where the image (Fig. 2) could be observed was limited by the values from $\sim 4 \times 10^3$ to $\sim 8 \times 10^3$ W/cm^2. At lower intensities it was impossible to discern single distinct bright spots against the background of quasiuniform illumination of the screen. At higher intensities the needle tips can be damaged, and such a damage more then once took place in the experiment. (It should be noted that the destruction of metal needles caused both by the mechanical stresses due to the applied intense electric fields and by a high emission current is common in FEM and FIM practice [9–12]).

The laser radiation intensity range in which the photoemission current could be measured quantitatively was limited also by a dynamic range of the registration system. This did not allow explicit determination of the dependence of the number of photoelectrons photoemitted in one bright spot $N_{\text{ph.e.}}$ by the laser radiation intensity I. It has been shown, however, that the photoemission current grows faster than the laser intensity. At the same time some dark spots (for example the dark spot at the left of Fig. 2) could be discerned throughout the laser radiation intensity range used.

For the interpretation of the observed photoelectron images, the following considerations may be

applied. Since a photoemitted electron has a certain nonzero kinetic energy of transverse motion $E_\perp$, every emitting center must be displayed as a circle with diameter [2,9–12]

$$d \simeq 2r\chi\sqrt{E_\perp / eU}\,. \qquad (4)$$

With $E_\perp \approx 1$ eV, $U = 2.5$ kV, $r = 600$ nm we obtain $d \approx 40$ nm which agrees satisfactorily with the dimensions of the individual bright spots in Fig. 2. The estimations show that the thermal heating of tips is not too high and cannot be responsible for stable electron emission. The photoemission from LiF crystals observed under visible light radiation must be caused by the photoionization of defects and/or impurities in their surface layers. (The photoeffect threshold of the LiF crystal matrix itself is about 10 to 11 eV [15,16].)

Since the visible radiation absorbing centers in the sample under study are mainly represented by F_2-centers (two adjacent anion vacancies capturing two electrons), it is logical to try to relate the bright spots observed in the photoelectron image to individual F_2-centers. Assuming that the depth of electron escape from the LiF crystal l_{esc} lies within 3 to 10 nm range [4,17,18], with the concentration of F_2-centers is $n \simeq 10^{16}$ cm^{-3} the average distance between the photoelectron images of these centers must be $L = (l_{esc} n)^{-1/2} = 100$ to 170 nm, i.e. a value of the same order as the distance between bright spots observed in the experiments.

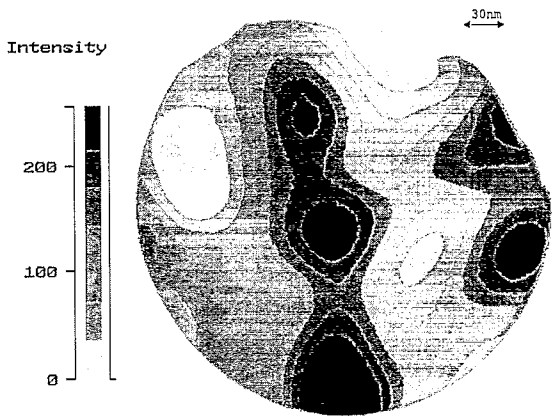

Fig. 2. Photoelectron image of the LiF:F_2 needle tip with the concentration of F_2-centers of $n \simeq 10^{16}$ cm^{-3}. The radius of the needle tip was $r \simeq 600$ nm; the tip is irradiated by all the spectral lines of Ar^+ laser with the intensity $I \simeq 5 \times 10^3$ W/cm^2. (Dark regions on correspond to the bright spots of photoelectron emission; see intensity scale).

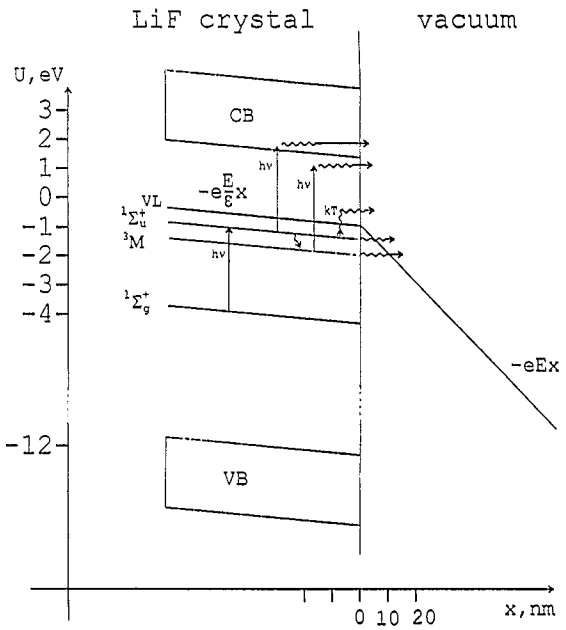

Fig. 3. Scheme of levels and transitions caused by laser irradiation of the F_2-centers in LiF crystals placed in the strong electric field of a projection microscope. Possible channels of F_2-center photoionization are indicated (see text).

Fig. 3 schematically shows the levels and transitions for F_2-centers of LiF crystals under laser irradiation. The following considerations apply:

- LiF crystals are characterized by a high negative electron affinity ~ -2.3 to 2.7 eV [19];
- F_2-centers can be photoionized in the crystal volume by absorption of two quanta of visible radiation [7,8,20];
- One quantum of visible radiation with an energy of 2.33 eV is not sufficient for an external photoeffect due to photoionization of F_2-centers which are close to the surface [5,6].

Thus the excited level Σ_u^+ of F_2-centers (the levels of F_2-centers are classified similarly to the levels of H_2 molecule [8]) lies near, most likely, somewhat lower than the vacuum level of LiF crystals. Ar^+ laser radiation is effectively absorbed in the transition $\Sigma_g^+ \rightarrow \Sigma_u^+$ (the transition lies in the range 400–500 nm, its maximum cross-section is at $\simeq 445$ nm). This leads to a population of the level Σ_u^+ with a radiative lifetime of $\tau \simeq 16$ ns and the metastable triplet level ^3M with a long lifetime [7,8].

Photoionization of F_2-centers may be initiated due to the absorption of one more quantum of laser radiation by an excited color center and, probably, due to tunnel or/and thermally stimulated electron emission from the ^{3}M level, in a strong electric field. The ultimate photoemission rate can be estimated from the formula

$$N \simeq \frac{I\sigma}{h\nu}, \tag{5}$$

which gives, with $I = 5 \times 10^3$ W/cm^2, $N \leq 10^6$ photoelectron/s. The numbers of photoelectrons observed in the experiment in one bright spot did not exceed this value even though in some cases they approached it.

The F_2^+-centers formed by photoionization of F_2-centers are already unstable at room temperature and they can be recharged to F_2-centers even in the absence of electric fields [8]. In strong electric fields this process must be much more effective, which should lead to the rapid recharging of these F_2^+-centers to their initial form, which can be photoionized once more by the incident laser radiation.

As fast as the observation of individual dark spots in the photoemission images of LiF:F_2 needle tips is concerned, it has to be noted that the presence of distinct dark spots is a phenomenon also observed in FEM and photoelectron images of metal tips [9–12]. The dark spots are associated with the presence of crystallographic low index planes with high work functions on the tip surfaces, the emission of electrons from these planes is more difficult. Most likely, some of the dark spots observed by us also can be associated with such low index planes and the regis-

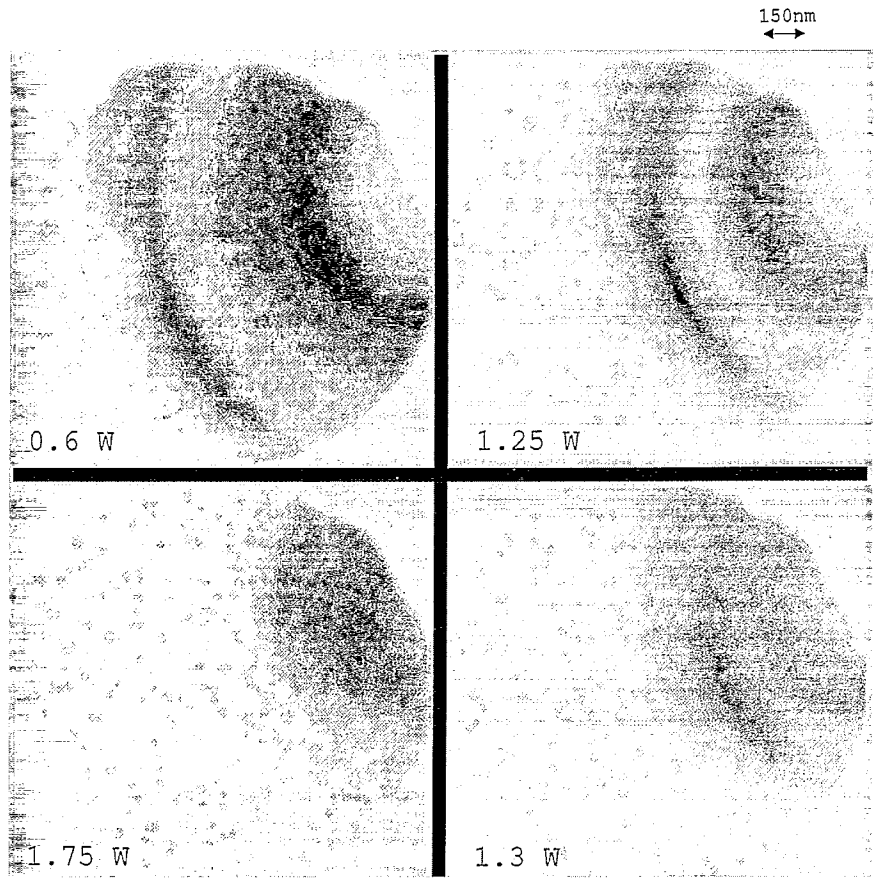

Fig. 4. A photoelectron image of the LiF:F_2^- needle tip, with a radius of curvature of $r \approx 3$ μm, obtained when the tip was irradiated by CW Ar^+ laser radiation at the 488 nm line. The potential applied to the needle is -500 V. The Ar^+ laser power used is indicated in quadrants: 600 mW corresponds to the irradiation intensity of $\sim 3 \times 10^3$ W/cm^2.

tered photoelectron image is defined by both the arrangement of photoemitting defects near the sample tip and the crystallographic structure of its surface. It should also be noted that the observation of dark spots in photoemission images indicates that the crystal surface studied is clean. It is well known that stable dark spots can be observed in FEM images of only sufficiently clean surfaces of metal tips [9–12].

Thus, the available experimental data do not contradict to the assumption that single individual F_2-centers can be observed in LiF crystals investigated with the use of a laser photoelectron projection microscope.

3.2. *LiF:F_2^- needles*

Besides LiF:F_2 crystals, we have also investigated photoelectron images of needle tips made of LiF:F_2^- crystals (some preliminary results of these samples studying were published in Ref. [21]). The concentration of F_2^--centers (these are F_2-centers having captured an additional electron) in the crystals under study was 1.4 to 2.5×10^{16} cm^{-3}, the concentration of F_2-centers in the same crystals was much higher, $n \simeq 10^{18}$ cm^{-3}. Such a high concentration of F_2-centers does not make it possible to realize such experimental conditions when visualization of individual photoemitting centers is possible. Indeed, there were no images similar to the one in Fig. 2 observed in the experiments with LiF:F_2^- crystals.

In these experiments, however, other interesting effects due to the possibility of strong heating of LiF:F_2^- crystals by laser radiation were observed. The point is that, due to high optical absorption of Ar^+ laser radiation by LiF:F_2^- crystals as compared with LiF:F_2 (their absorption factors at $\lambda = 488$ nm being ~ 100 and ~ 1 cm^{-1} respectively) the tips of these needles can be heated to several hundreds of degrees or even melted by incident laser radiation (the studies of the tips of all LiF:F_2^- needles after experiments on them showed that the tips were really melted: their radius of curvature increased up to 3 to 4 μm, and their tips were nearly ideal spheres in shape). Such heating, of course, and especially their transformation to melted or premelted states can and must change essentially the whole structure of the LiF crystal lattice that makes the observation of individual defects of such objects rather meaningless but, in return, it is possible to apply laser photoelectron microscopy to study relevant "large-scale" changes in the crystal structure. (Note that F_2^--centers become thermally unstable even when the LiF crystal is slightly heated [7,8,22].)

In our opinion, the photoelectron images of LiF:F_2^- needle tips presented in Fig. 4 can be interpreted as the observation of such structural reconstruction of a LiF crystal in a strong electric field under laser irradiation heating. The central dark photoemission spot is beyond the area of vision of the photoelectron projector and should be in the right upper angle of the figures (it has been noticed above that just a comparatively small part of the needle tip can be observed by our photoelectron microscope), and we are able to observe bright circles of different diameter that are concentric with this center. The position and the diameter of these circles depended on the laser radiation intensity on the tip and the potential applied to the needle U. By varying these parameters we could easily "move" the concentric circles along the whole field of vision of the microscope – see Fig. 4. These replacements are quite reversible and the observed pattern demonstrates surprising stability throughout several hours.

We think that the effects observed are in compliance with the effect of thermal faceting of metal needle tips which is well-known and long-studied in FIM [9–12,23]. It has been found that metals in premelted state are prone to form so-called hill and valley structures which are really parallel chains of defects and a more or less perfect planes characterized by low Miller indices formed between them. For spherical monocrystals of metals and semispherical tips of FIM needles such hill and valley structures usually form circles concentric with the existing low indices planes, with the needle tip in particular (see Ref. [23] and references cited therein). Since it is the defects in the crystalline structure of wide-gap LiF crystal that are responsible for the photoemission while the crystal is irradiated by visible light, thermal faceting of LiF:F_2^- crystals must manifest itself just as it appears in Fig. 4, i.e. in the form of bright circles concentric with the center of the needle tip. Between them there are dark areas with a small concentration of defects. (It must be noted that low index planes correspond to dark spots in FEM and photoelectron images.)

4. Conclusions

We have developed a laser photoelectron projection microscope and investigated the photoelectron images of LiF:F_2 and LiF:F_2^- needle tips observed while the tips are exposed to CW Ar^+ laser radiation. A magnification of 10^5 and a spatial resolution of up to 30 nm have been obtained which is sufficient to visualize individual defects in LiF crystals with concentration $n \leq 10^{17}$ cm^{-3}. Also, the effects of thermal faceting of LiF:F_2^- needle tips heated by laser radiation were for the first time observed.

Our studies can be considered as the first successful realization of the earlier suggested by us method of laser resonant photoelectron microscopy characterized by an ultra high spatial resolution and chemical selectivity at the same time [2,3].

Acknowledgements

We thank Professor T.T. Basiev for the supply of LiF:F_2 and LiF:F_2^- crystal specimens and useful discussions and Hamamatsu Photonics K.K for lending us the necessary instrumentation. We are also grateful to the Russian Foundation for Fundamental Research and Department of Defence (USA) for their financial support.

References

[1] O.H. Griffith and G.F. Rempfer, Adv. Opt. Electron Microsc. 10 (1987) 269.
[2] V.S. Letokhov, Kvant. Electr. 2 (1975) 930 (in Russian).
[3] V.S. Letokhov and S.K. Sekatskii, Appl. Phys. B 55 (1992) 177.
[4] A.B. Aleksandrov, E.D. Aluker, I.A. Vasil'ev, A.F. Nechaev and S.A. Chernov, Introduction to Radiational Physics and Chemistry of Alkaline–Haloid Crystals Surface (Zinatne, Riga, 1989) (in Russian).
[5] V.S. Letokhov and S.K. Sekatskii, Opt. Spectrosk. 76 (1994) 303 (in Russian).
[6] S.K. Sekatskii, V.S. Letokhov, T.T. Basiev and V.V. Ter-Mikirtychev, Appl. Phys. A 58 (1994) 467.
[7] T.T. Basiev, S.B. Mirov and V.V. Osiko, IEEE J. Quantum Electron. QE-24 (1988) 1052.
[8] A.I. Nepomnyashchkih, E.A. Radzabov and A.V. Egnanov, Color Centers and Luminescence in LiF Crystals (Nauka, Novosibirsk, 1984).
[9] R. Gomer, Field Emission and Field Ionization (Harvard University Press, Cambridge, MA, 1961).
[10] E.W. Müller and T.T. Tsong, Field Ion Microscopy: Principles and Applications (Elsevier, Amsterdam, 1969).
[11] M.K. Miller and G.D.W. Smith, Atom Probe Microanalysis: Principles and Applications to Materials Problems (OX1 3PH, Oxford, 1989).
[12] J.A. Panitz, Meth. Exp. Phys. 53 (1985) 350.
[13] G.L. Kellogg, J. Appl. Phys. 53 (1992) 6383.
[14] S.C. Jain and G.P. Sootha, Phys. Status Solidi 22 (1967) 505.
[15] R.T. Poole, J. Liesegand, R.C.G. Leckey and J.G. Jenkin, Chem. Phys. Lett. 23 (1973) 194.
[16] W. Pong and C.S. Inouye, J. Electron Spectrosc. Rel. Phen. 11 (1977) 165.
[17] A.A. Maiste, A.M.E. Saar, B.A. Sarkin and M.A. Elango, Opt. Spectrosk. 38 (1975) 738 (in Russian).
[18] B. Quirim, W. Schwarz, Z. Wu et al., Appl. Phys. Lett. 60 (1992) 1831.
[19] D.A. Lapiano-Smith, E.A. Eklund, F.J. Himpsel and L.J. Terminello, Appl. Phys. Lett. 59 (1991) 2174.
[20] T.T. Basiev, S.B. Mirov and V.V. Ter-Mikirtychev, Proc. SPIE 227 (1991) 1839.
[21] V.N. Konopsky, S.K. Sekatskii and V.S. Letokhov, Pis'ma Zh. Eksp. Teor. Fiz. 60 (1994) 691 (in Russian).
[22] W. Osten and W. Waidelich, Z. Phys. 178 (1964) 244.
[23] G.G. Summers and H.N. Southworth, Surf. Sci. 53 (1975) 583.